

Supporting Information for

**Spiro[pyrrol-benzopyran] Based Probe with High
Asymmetry for Chiroptical Sensing via Circular
Dichroism**

Jingyun Tan,^a Chunfei Wang,^a Hio Kuan Lao,^a Wenjing Wang,^{*,b} Gang Feng,^a
Daqiang Yuan,^b Changfeng Wu,^c Xuanjun Zhang^{*,a}

Table of Contents

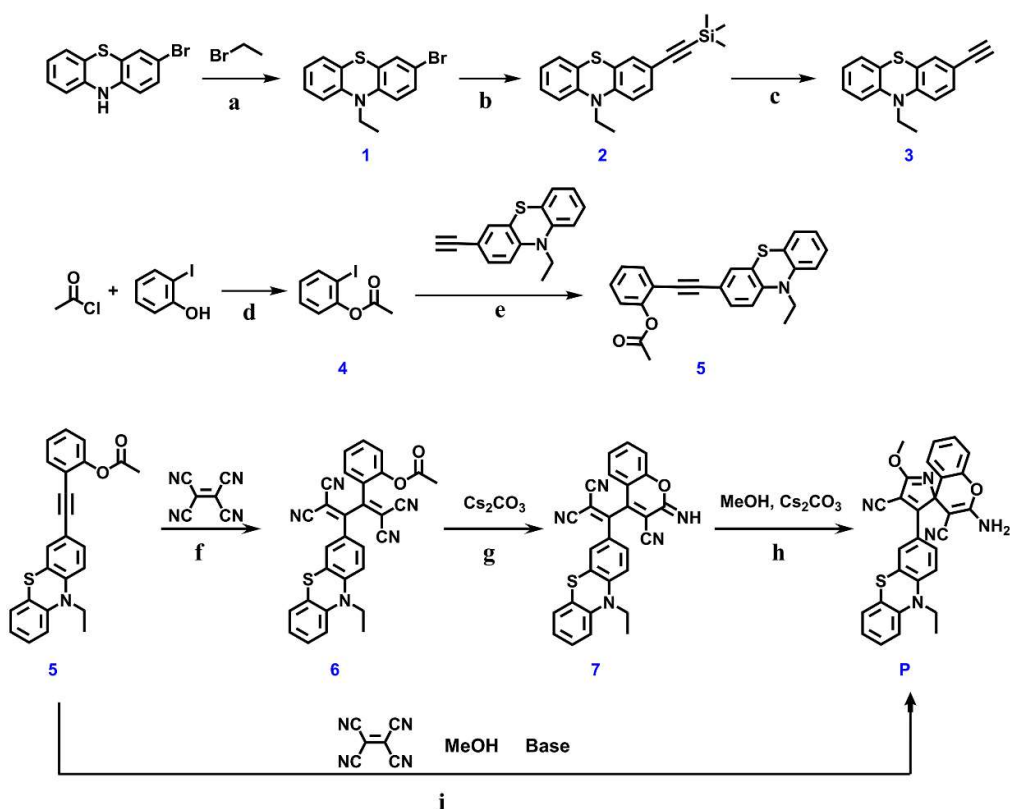
Table of Contents	1
Experimental Procedures	3
Scheme S1. The synthetic routes of intermediates and target products.	3
Figure S1. Chiral HPLC chromatogram of a) the crude sample P and b) c) two enantiomers after separation (P1 and P2).	5
Results and Discussion	6
1. Crystallography Results.	6
Figure S2. ORTEP diagram of P with atom labels and 50% probability displacement ellipsoids for non-H atoms.	6
Table S1. Crystal data and structure refinement for P.	6
Table S2. Selected bond distances (Å) and angles (°) for P.	7
2. Detection towards hypochlorite.	8
Figure S3. Mass spectra of P before and after adding hypochlorite (PDO).	8
Figure S4. CD spectrum of P1 (20 uM) toward different concentration of hypochlorite.	9
Figure S5. CD spectrum of P2 (20 uM) toward different concentration of hypochlorite.	9
Figure S6. Dissymmetry Factor g_{CD} of P1, P2, P1DO and P2DO.	10
Figure S7. Selected frontier molecular orbits of P and PDO around 250 and 280 nm (TD-DFT/b3lyp).	11
Figure S8. UV-vis spectrum of P2 (20 uM) toward different species of ROS/RNS.	11
Figure S9. CD spectrum of P2 (20 uM) toward different species of ROS/RNS.	12
Figure S10. UV-vis spectrum of P2 (20 uM) in solution with different pH value.	12
Figure S11. CD spectrum of P2 (20 uM) in solution with different pH value.	13
¹H NMR and ¹³C NMR Spectra.	14
Figure S12. ¹ H NMR spectrum of 1 in acetone-d ₆	14
Figure S13. ¹³ C NMR spectrum of 1 in DMSO-d ₆	14
Figure S14. ¹ H NMR spectrum of 2 in acetone-d ₆	15
Figure S15. ¹³ C NMR spectrum of 2 in DMSO-d ₆	15
Figure S16. ¹ H NMR spectrum of 3 in DMSO-d ₆	16

Figure S17. ^{13}C NMR spectrum of 3 in DMSO-d_6 .	16
Figure S18. ^1H NMR spectrum of 4 in CDCl_3 .	17
Figure S19. ^1H NMR spectrum of 5 in DMSO-d_6 .	17
Figure S20. ^{13}C NMR spectrum of 5 in DMSO-d_6 .	18
Figure S21. ^1H NMR spectrum of 6 in DMSO-d_6 .	18
Figure S22. ^{13}C NMR spectrum of 6 in DMSO-d_6 .	19
Figure S23. ^1H NMR spectrum of 7 in DMSO-d_6 .	19
Figure S24. ^{13}C NMR spectrum of 7 in DMSO-d_6 .	20
Figure S25. ^1H NMR spectrum of P in DMSO-d_6 .	20
Figure S26. ^{13}C NMR spectrum of P in DMSO-d_6 .	21
MS spectra.	21
Figure S27. Mass spectra of 5.	21
Figure S28. Mass spectra of 6.	22
Figure S29. Mass spectra of 7.	22
Figure S30. Mass spectra of P.	23
References	23

Experimental Procedures

General. Starting materials were commercially available and were used without purification. All solvents for reactions and spectral measurement were purified by conventional methods before use. The NMR spectra were recorded at 25 °C on a Bruker Avance 400 spectrometer, and the chemical shift are reported as parts per million from TMS (δ). Coupling constants J are given in Hertz. Elemental analyses were performed with a Perkin Elmer 240C elemental analyzer, three times averaged. Mass spectra were determined with the ESI mass spectra which were recorded on the Waters Xevo G2-XS QToF matrix-assisted time of flight mass spectrometer. The single crystal data was recorded with a Bruker SMART APEX-II CCD detector using graphite monochromated Cu-K α radiation. Chiral HPLC was performed on an Agilent Technologies 1200 infinity system equipped Daicel CHIRALPAK IA columns (250*4.6 mm). UV-vis absorption spectra and circular dichroism (CD) spectra were measured on a Chirascan from Applied Photophysics. The g factor g_{CD} is the ratio of molar CD to molar extinction coefficient (for unpolarized ligh), $g_{CD} = \Delta\epsilon(\lambda)/\epsilon(\lambda)$ [1], where $\Delta\epsilon(\lambda)$ is the molar circular dichroism, $\Delta\epsilon(\lambda) = \epsilon_L(\lambda) - \epsilon_R(\lambda)$; $\epsilon(\lambda) = 1/2 * [\epsilon_L(\lambda) + \epsilon_R(\lambda)]$.

Computational Section. All the quantum chemical computations have been carried out with Gaussian 03 software (Gaussian, Inc., Pittsburgh, PA, 2003). The conformational search was performed by Spartan's 14 using Merck Molecular Force Field (MMFF) level. The low energy conformations (Boltzmann distribution ≥ 5.0 %) of compounds were submitted to the density functional theory (DFT) optimization at the level of b3lyp/6-31g(d,p), using the pcm solvation model with the dielectric constant representing H₂O. The optimized structures were subject to the frequency calculations at b3lyp/6-31g(d,p) level to confirm the true energy minimal located and generate the thermodynamic data. The optimized structures were further submitted to the Time-dependent density functional theory (TDDFT) calculations at b3lyp/6-31g(d,p). CD values were read and Boltzman averaged using the SpecDis 1.53.



Scheme S1. The synthetic routes of intermediates and target products.

Synthesis of **1**. Bromoethane (4.9037 g, 45 mmol) and 3-bromophenothiazine (8.3450 g, 30 mmol) was dissolved in DMSO (150 mL) under N₂ atmosphere, and then KOH (4.9708 g, 89 mmol) was added slowly. The mixed solution was stirred overnight under room temperature. The mixture was diluted with deionized water (200 mL), and then extracted with ethyl acetate (3 x 150 mL). The organic phase was dried with MgSO₄ and concentrated. The crude was purified via column chromatography on silica gel. The product is white solid, with yield 9.0000 g, 98%. ¹H NMR (400 MHz, Acetone-d₆) δ 7.34 (dd, $J = 8.7, 2.3$ Hz, 1H), 7.28 (d, $J = 2.3$ Hz, 1H),

7.23 (ddd, $J = 8.2, 7.3, 1.6$ Hz, 1H), 7.15 (dd, $J = 7.6, 1.5$ Hz, 1H), 7.04 (dd, $J = 8.3, 1.1$ Hz, 1H), 6.97 (td, $J = 7.6, 1.3$ Hz, 2H), 3.99 (q, $J = 6.9$ Hz, 2H), 1.38 (t, $J = 6.9$ Hz, 3H); ^{13}C NMR (101 MHz, DMSO) δ 144.45, 144.28, 130.54, 129.28, 128.34, 127.59, 126.05, 123.17, 122.65, 117.50, 116.11, 114.07, 41.65, 12.96.

Synthesis of **2**. Triphenylphosphine (0.0472 g, 0.18 mmol) was dissolved in THF/Et₃N (v/v=15 mL / 15 mL), and the solution was degassed with nitrogen for 0.5 h. The reactant and catalyst were added sequentially, trimethylsilylacetylene (0.8 mL, 5.30 mmol), **1** (0.5420 g, 1.77 mmol), CuI (0.0202 g, 0.11 mmol), PdCl₂(PPh₃)₂ (0.0746 g, 0.11 mmol). The mixed suspension was reacted under 60°C for 1 day. The yellow solution turned dark red gradually. When the reaction finished, the mixture was filtrated. Concentrated the solution, and the obtained residual was purified via column chromatography on silica gel (Hexane/Ethyl acetate=15/1). The product was yellow solid, with yield 0.3890 g, 68%. ^1H NMR (400 MHz, Acetone-*d*₆) δ 7.05 (dd, $J = 8.5, 2.0$ Hz, 1H), 6.99 (td, 1H), 6.96 (d, $J = 2.0$ Hz, 1H), 6.91 (dd, $J = 7.6, 1.5$ Hz, 1H), 6.80 (dd, $J = 8.3, 1.1$ Hz, 1H), 6.77 – 6.70 (m, 2H), 3.69 (q, $J = 6.9$ Hz, 2H), 1.07 (t, $J = 6.9$ Hz, 3H), 0.00 (s, 9H); ^{13}C NMR (101 MHz, DMSO) δ 144.36, 142.98, 130.83, 129.04, 127.33, 126.59, 122.53, 122.37, 121.60, 115.28, 115.19, 114.73, 104.15, 93.26, 40.78, 12.00, -0.50.

Synthesis of **3**. **2** (0.3230 g, 1.00 mmol) and K₂CO₃ (0.4150 g, 3.00 mmol) were added into methanol (100 mL), and the mixture was stirred under room temperature overnight. Reduce the reaction solution in vacuo and then dissolve in ethyl acetate, followed by washing with brine. The organic layer was collected and concentrated in vacuo. The crude residual was purified using silical gel chromatography (Hexane/Ethyl acetate=15/1). The product was yellow solid, with yield 0.2130 g, 85%. ^1H NMR (400 MHz, DMSO-*d*₆) δ 7.31 (dd, $J = 8.4, 2.0$ Hz, 1H), 7.25 – 7.20 (m, 2H), 7.15 (dd, $J = 7.6, 1.6$ Hz, 1H), 7.05 (dd, $J = 8.3, 1.1$ Hz, 1H), 7.01 – 6.95 (m, 2H), 4.18 – 4.09 (s, 1H), 3.93 (q, $J = 6.9$ Hz, 2H), 1.31 (t, $J = 6.9$ Hz, 3H). ^{13}C NMR (101 MHz, DMSO) δ 145.31, 144.06, 131.82, 130.13, 128.31, 127.56, 123.56, 123.31, 122.57, 116.15, 115.83, 115.79, 83.29, 80.96, 41.70, 12.97.

Synthesis of **4**. **4** was synthesized by literature procedures.^[2] ^1H NMR (400 MHz, Chloroform-*d*) δ 7.82 (dt, $J = 5.7, 2.9$ Hz, 1H), 7.35 (td, 1H), 7.09 (dd, $J = 8.1, 1.5$ Hz, 1H), 6.97 (td, $J = 7.8, 1.5$ Hz, 1H), 2.36 (s, 3H).

Synthesis of **5**. **5** was obtained by the reaction between **3** and **4** via procedure similar with **2**. The product is yellow powder, with yield of 52 %. ^1H NMR (400 MHz, DMSO-*d*₆) δ 7.59 (dd, $J = 7.7, 1.7$ Hz, 1H), 7.50 – 7.40 (td, $J = 7.4, 1.1$ Hz, 1H), 7.38 – 7.27 (m, 2H), 7.28 – 7.17 (m, 3H), 7.14 (dd, $J = 7.6, 1.5$ Hz, 1H), 7.07 – 6.99 (m, 2H), 6.96 (td, $J = 7.4, 1.1$ Hz, 1H), 3.93 (q, $J = 6.9$ Hz, 2H), 2.36 (s, 3H), 1.30 (t, $J = 6.9$ Hz, 3H). ^{13}C NMR (101 MHz, DMSO) δ 169.09, 151.57, 145.43, 143.95, 132.90, 131.60, 130.31, 129.66, 128.33, 127.58, 126.72, 123.70, 123.39, 123.17, 122.50, 117.29, 116.17, 115.92, 93.89, 84.68, 41.78, 21.04, 12.97. Q-TOF *m/z*: calcd, 385.1136; found, 386.1312 [M+H]⁺.

Synthesis of **6**. **5** (0.8866 g, 2.30 mmol) was mixed with tetracyanoethylene (0.3540 g, 2.70 mmol) in acetonitrile (30 mL) while stirring. The mixture was reacted for 6 h under 60°C. The dark brown reaction mixture was concentrated in vacuum, and the residual was purified using flash silical gel chromatography (Hexane/Ethyl acetate=1/1). The product is black powder, with yield 1.0631 g, 90%. ^1H NMR (400 MHz, DMSO-*d*₆) δ 7.95 (d, $J = 8.0$ Hz, 1H), 7.75 – 7.64 (m, 2H), 7.59 (s, 1H), 7.47 (t, 1H), 7.40 (d, $J = 8.4$ Hz, 1H), 7.23 (t, $J = 7.7$ Hz, 1H), 7.17 – 7.06 (m, 3H), 7.02 (t, $J = 7.5$ Hz, 1H), 3.98 (q, $J = 6.9$ Hz, 2H), 2.32 (s, 3H), 1.29 (t, $J = 6.9$ Hz, 3H). ^{13}C NMR (101 MHz, DMSO) δ 168.67, 163.80, 162.30, 148.45, 141.91, 135.21, 132.22, 131.65, 128.68, 127.67, 126.92, 124.80, 124.61, 123.27, 121.41, 116.87, 115.58, 113.74, 113.04, 112.40, 112.08, 95.12, 83.10, 42.44, 21.52, 12.76. Q-TOF *m/z*: calcd, 513.1259; found, 514.1324 [M+H]⁺.

Synthesis of **7**. **6** (0.1284 g, 0.25 mmol) was dissolved in dimethyl sulfoxide (10 mL), and then added Cs₂CO₃ (0.1642 g, 0.50 mmol). The mixture was stirred for 3 h under room temperature. The reaction mixture was diluted in water and extracted 3 times with dichloromethane. The organic layer was concentrated, and the obtained crude residual was purified using flash silical gel chromatography (Hexane/Ethyl acetate=5/1). The product is red powder, with yield 0.0719 g, 45%. ^1H NMR (400 MHz, DMSO-*d*₆) δ 8.08 – 8.01 (d, 1H), 7.79 (ddd, $J = 8.5, 7.1, 1.3$ Hz, 1H), 7.27 – 7.14 (m, 5H), 7.12 (dd, $J = 7.7, 1.5$ Hz, 1H), 7.04 – 6.96 (m, 3H), 6.94 (t, $J = 7.2$ Hz, 1H), 3.89 (q, $J = 6.8$ Hz, 2H), 1.28 (t, $J = 6.9$ Hz, 3H). ^{13}C NMR (101 MHz, DMSO) δ 174.71, 173.36, 166.64, 145.40, 144.11, 140.01, 130.35, 128.24, 127.81, 127.55, 127.36, 126.55, 126.22, 125.95, 123.13, 122.86, 122.71, 122.67, 120.05, 115.99, 115.43, 114.55, 113.42, 112.70, 104.98, 71.65, 41.59, 12.98. Q-TOF *m/z*: calcd, 471.1154; found, 472.0623 [M+H]⁺.

Synthesis of **P** (method 1). **7** (0.1178 g, 0.25 mmol) was dissolved in methanol (15 mL), and then added Cs₂CO₃ (0.1642 g, 0.50 mmol). The reddish-brown solution turns to yellow. The mixture was stirred under room temperature for 3 h. The reaction mixture was concentrated in vacuum, and dispersed in dichloromethane, followed by washing 3 times with brine. The organic layer was concentrated, and the obtained crude residual was purified using flash silical gel chromatography (Dichloromethane). The product is red powder, with yield 0.1195 g, 95%. ^1H NMR (400 MHz, DMSO-*d*₆) δ 7.46 – 7.41 (m, 3H), 7.38 (ddd, $J = 8.6, 7.2, 1.7$ Hz, 1H), 7.26 (d, $J = 2.3$ Hz, 1H), 7.24 – 7.17 (m, 2H), 7.13 – 7.01 (m, 4H), 6.96 (qd, $J = 7.7, 1.3$ Hz, 2H), 3.95 – 3.87 (m, 5H), 1.26 (t, $J = 6.9$ Hz, 3H). ^{13}C NMR (101 MHz, DMSO) δ 176.60, 165.47, 161.00, 148.31, 147.73, 142.68, 130.75, 128.58, 128.49, 127.62, 127.24, 125.88, 125.77, 123.96, 123.42, 122.65, 121.37, 118.80, 117.91, 117.24, 116.39, 115.69, 114.30, 100.15, 74.26, 56.74, 54.72, 41.98, 12.80. Anal. Calcd for C₂₉H₂₁N₅O₂S (503.58): C, 69.17%; H, 4.20%; N, 13.91%; found: C, 69.20%; H, 4.19%; N, 13.93%. Q-TOF *m/z*: calcd, 503.1416; found,

504.1614 [M+H]⁺. Synthesis of **P** (method 2). **P** was obtained directly by mixing **5** (0.1386 g, 0.36 mmol), tetracyanoethylene (0.0550 g, 0.43 mmol), THF (15 mL, or DMSO 10 mL), cesium carbonate (0.2610 g, 0.80 mmol) and MeOH (15 mL) under 60°C for 10 h. The reaction mixture was concentrated in vacuum, and dispersed in dichloromethane, followed by washing 3 times with brine. The organic layer was concentrated, and the obtained crude residual was purified using flash silica gel chromatography (Dichloromethane). The product is red powder, with yield 0.1360 g, 70%. When the base was changed from carbonate to triethylamine, sodium hydrogen carbonate and potassium carbonate, the reaction yield is 0%, 63%, 69%, respectively. Enantiomers of **P** were separated via Chiral HPLC, which was performed on an Agilent Technologies 1200 infinity system, monitored at 400 nm. Mixed solvent (CH₃CN/H₂O=7/3) was used as eluent, flow rate was 1.0 mL/min. Finally two enantiomers **P1** and **P2** could be obtained (Figure S1).

Comparison of two pathways for the product **P** (method 1 and method 2). Method 1 is a kind of controlled stepwise reaction that starting from **5**, going through three steps (reaction f, g and h), and finally product generates. Since intermediate **7** is not stable enough, the yield of reaction g is unsatisfactory. The one-pot multicomponent reaction is a good solution for this difficulty, which consumes less reaction time and avoid tedious labor for purification, and most of all, the yield of 70% is higher than the overall yield of method 1 (38%).

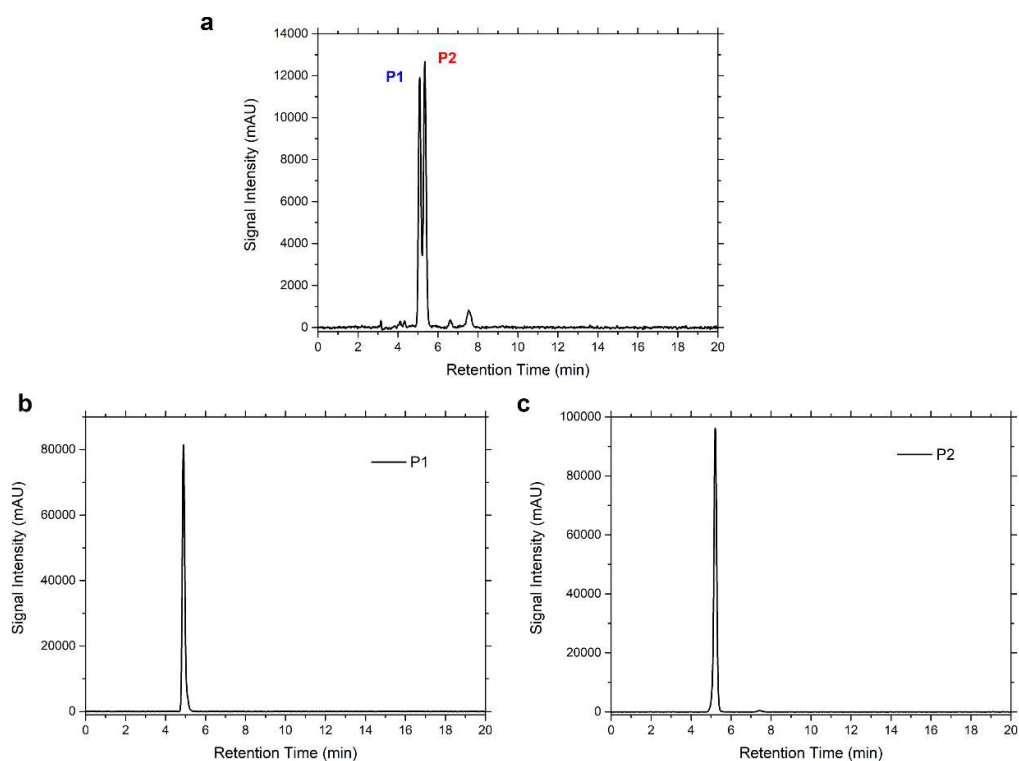


Figure S1. Chiral HPLC chromatogram of a) the crude sample **P** and b) c) two enantiomers after separation (**P1** and **P2**).

Results and Discussion

1. Crystallography Results.

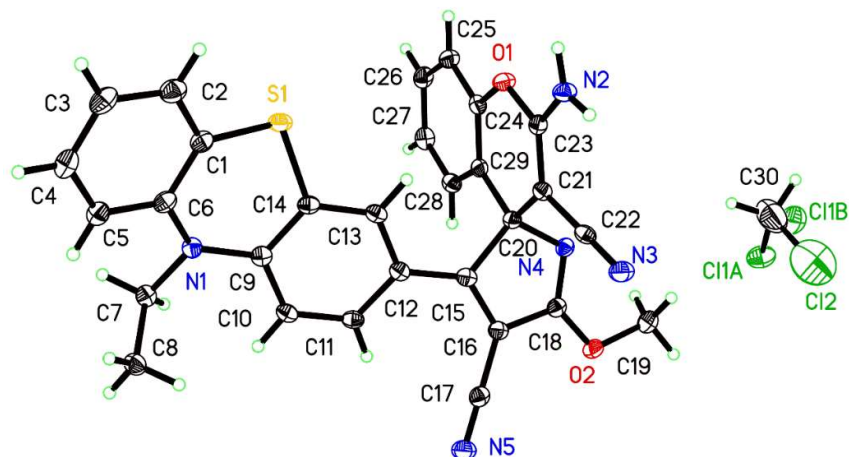


Figure S2. ORTEP diagram of **P** with atom labels and 50% probability displacement ellipsoids for non-H atoms.

(The crystal was obtained by slow recrystallization from mixed solution dichloromethane/toluene for 3 days. Solvent molecule dichloromethane shows slight disorder)

Table S1. Crystal data and structure refinement for **P**.

Identification code (CCDC No.)	1887556
Empirical formula	C _{29.50} H ₂₂ ClN ₅ O ₂ S
Formula weight	546.03
Temperature (K)	293(2)
Wavelength (Å)	1.54184
Crystal system	triclinic
Space group	<i>P</i> -1
Unit cell dimensions (Å, °)	<i>a</i> = 8.0089(2); α = 82.255(3) <i>b</i> = 12.1459(4); β = 80.785(2) <i>c</i> = 13.9061(4); γ = 79.244(3)
Volume (Å ³)	1304.11(7)
<i>Z</i>	2
Calculated density (g cm ⁻³)	1.391
Absorption coefficient (mm ⁻¹)	2.354
<i>F</i> ₀₀₀	566
Reflections collected	21033
Independent reflections	5161 [<i>R</i> _{int} = 0.0215]
Completeness to θ_{\max} (%)	0.979
Max. and min. transmission	and
Refinement method	Full-matrix least-squares on <i>F</i> ²

Data / restraints / parameters	5161 / 0 / 373
Goodness-of-fit on F^2	1.033
Final R indices [$I > 2\sigma(I)$]	$R1 = 0.0577$, $wR2 = 0.1661$
R indices (all data)	$R1 = 0.0593$, $wR2 = 0.1679$
Largest diff. peak and hole ($e \text{ \AA}^{-3}$)	1.319 and -1.592

Table S2. Selected bond distances (\AA) and angles ($^\circ$) for **P**.

S(1)-C(1)	1.764(2)	C(20)-C(29)	1.514(4)
S(1)-C(14)	1.760(2)	C(14)-S(1)-C(1)	100.01(11)
O(1)-C(23)	1.359(3)	C(6)-N(1)-C(7)	118.86(18)
O(1)-C(24)	1.387(3)	C(9)-N(1)-C(6)	121.78(18)
O(2)-C(18)	1.329(3)	C(18)-N(4)-C(20)	106.55(18)
O(2)-C(19)	1.442(3)	N(4)-C(20)-C(15)	105.33(17)
N(1)-C(6)	1.417(3)	N(4)-C(20)-C(21)	107.55(16)
N(1)-C(7)	1.474(3)	N(4)-C(20)-C(29)	110.12(17)
N(4)-C(18)	1.282(3)	C(21)-C(20)-C(15)	111.32(17)
N(4)-C(20)	1.484(3)	C(29)-C(20)-C(15)	112.36(17)
N(5)-C(17)	1.153(3)	C(29)-C(20)-C(21)	109.96(17)
C(15)-C(16)	1.358(3)	N(3)-C(22)-C(21)	179.7(2)
C(15)-C(20)	1.540(3)	N(2)-C(23)-O(1)	110.61(18)
C(20)-C(21)	1.522(3)	C(29)-C(24)-O(1)	122.97(19)

2. Detection towards hypochlorite.

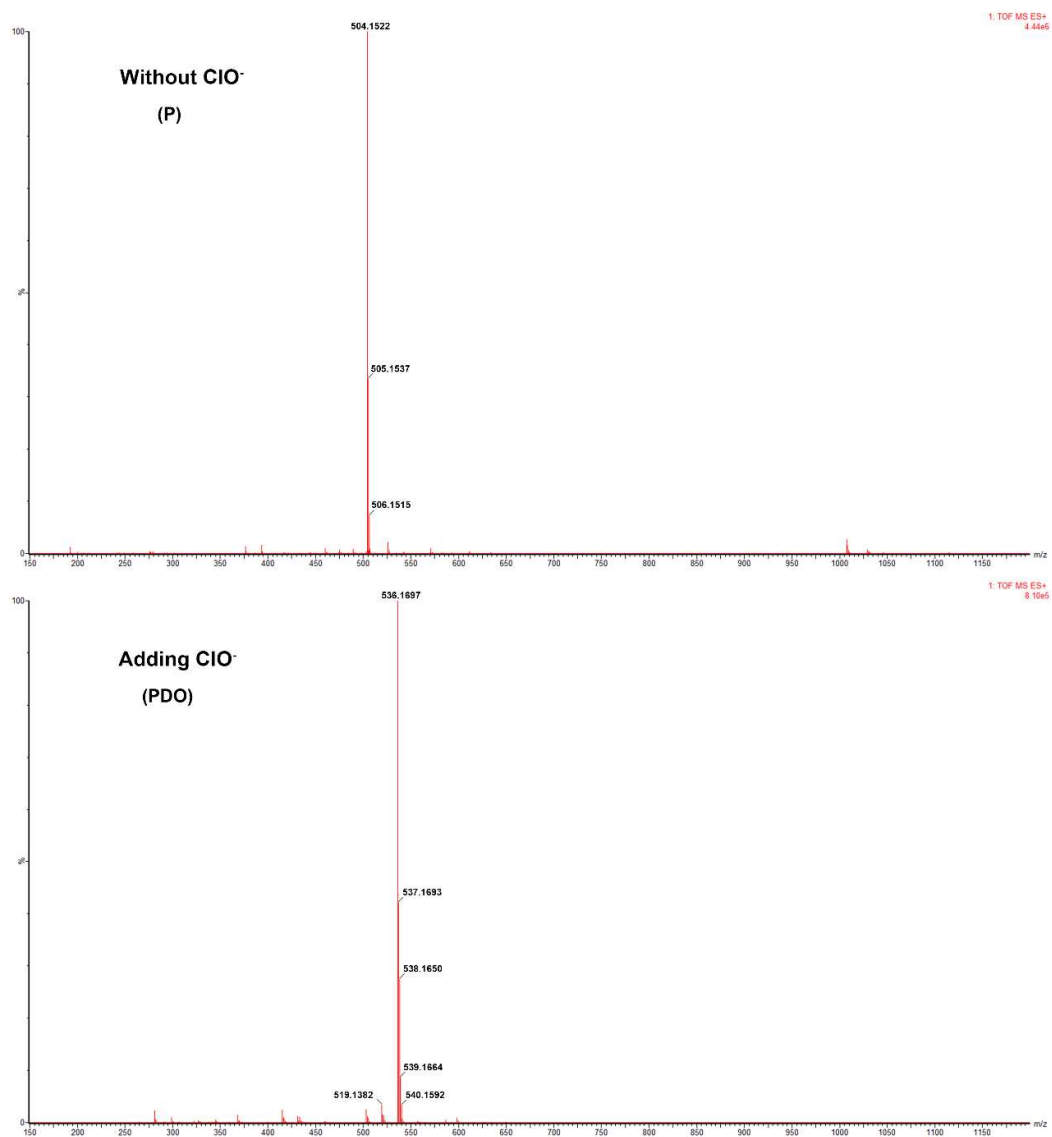


Figure S3. Mass spectra of P before and after adding hypochlorite (PDO).

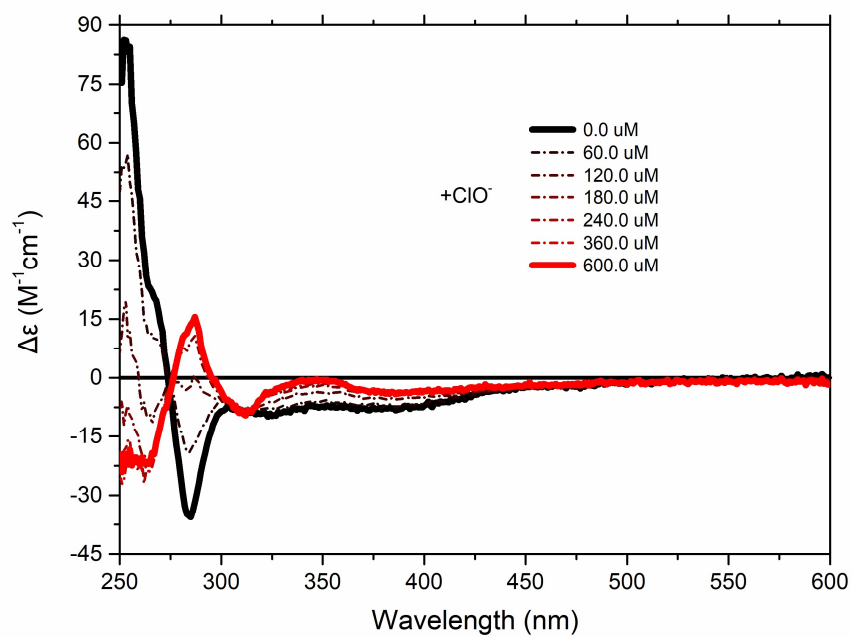


Figure S4. CD spectrum of P1 (20 uM) toward different concentration of hypochlorite.

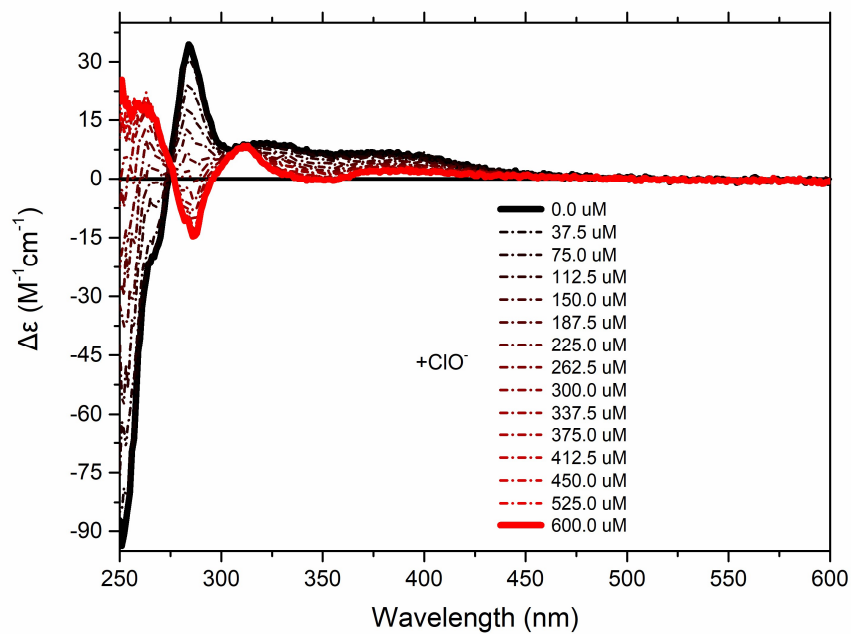


Figure S5. CD spectrum of P2 (20 uM) toward different concentration of hypochlorite.

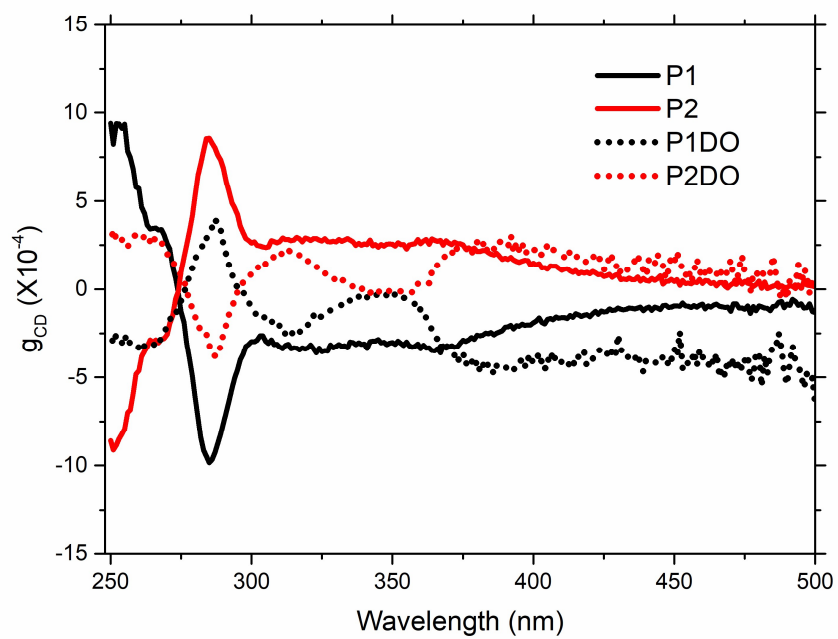


Figure S6. Dissymmetry Factor g_{CD} of P1, P2, P1DO and P2DO.

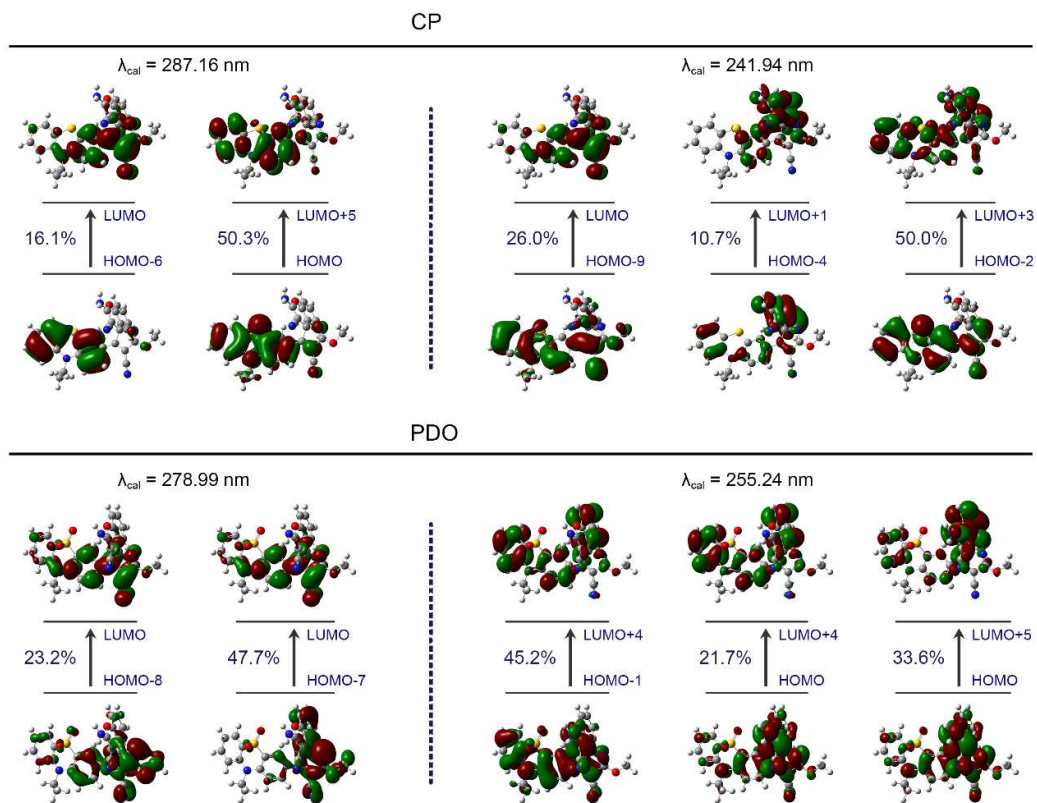


Figure S7. Selected frontier molecular orbitals of **P** and **PDO** around 250 and 280 nm (TD-DFT/b3lyp).

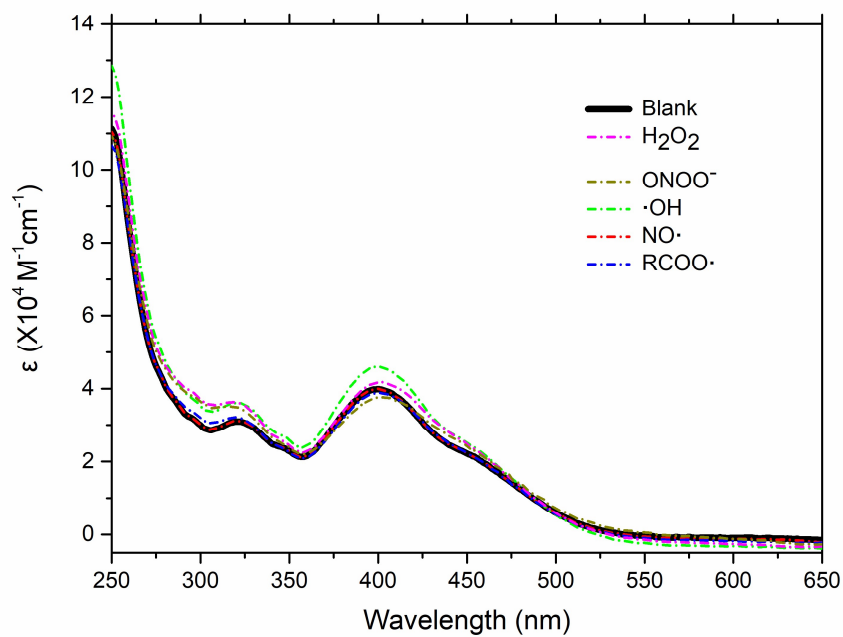


Figure S8. UV-vis spectrum of **P2** (20 μM) toward different species of ROS/RNS.

(The concentration of H_2O_2 , ONOO^- , $\cdot\text{OH}$, $\text{NO}\cdot$ and $\text{RCOO}\cdot$ is 100 μM , 50 μM , 50 μM , 50 μM and 50 μM , respectively)

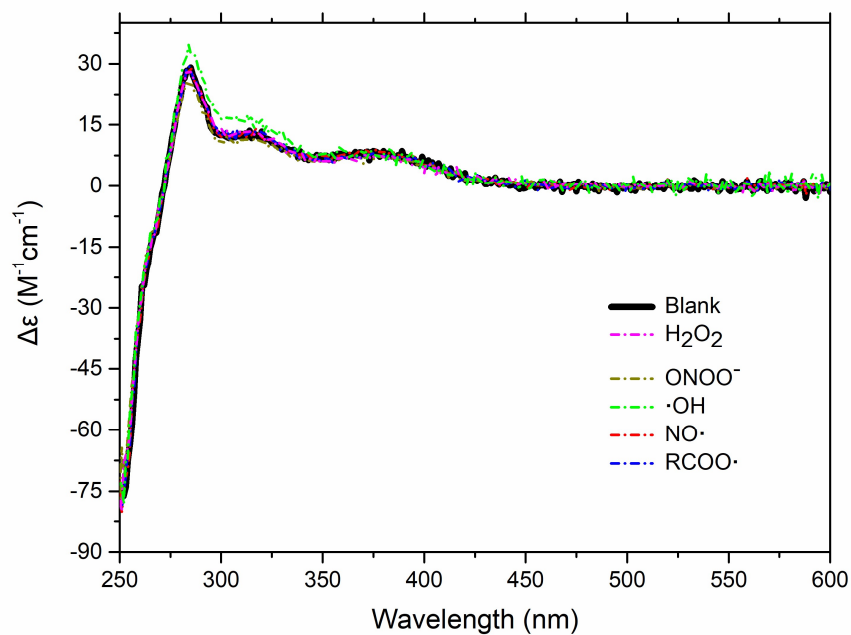


Figure S9. CD spectrum of **P2** (20 μM) toward different species of ROS/RNS. (The concentration of H_2O_2 , ONOO^- , $\cdot\text{OH}$, $\text{NO}\cdot$ and $\text{RCOO}\cdot$ is 100 μM , 50 μM , 50 μM , 50 μM and 50 μM , respectively)

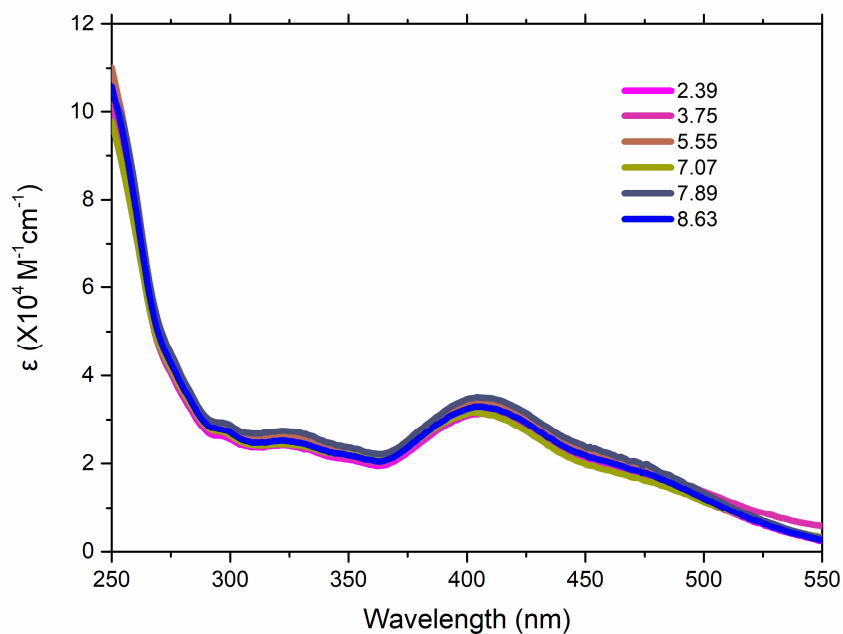


Figure S10. UV-vis spectrum of **P2** (20 μM) in solution with different pH value.

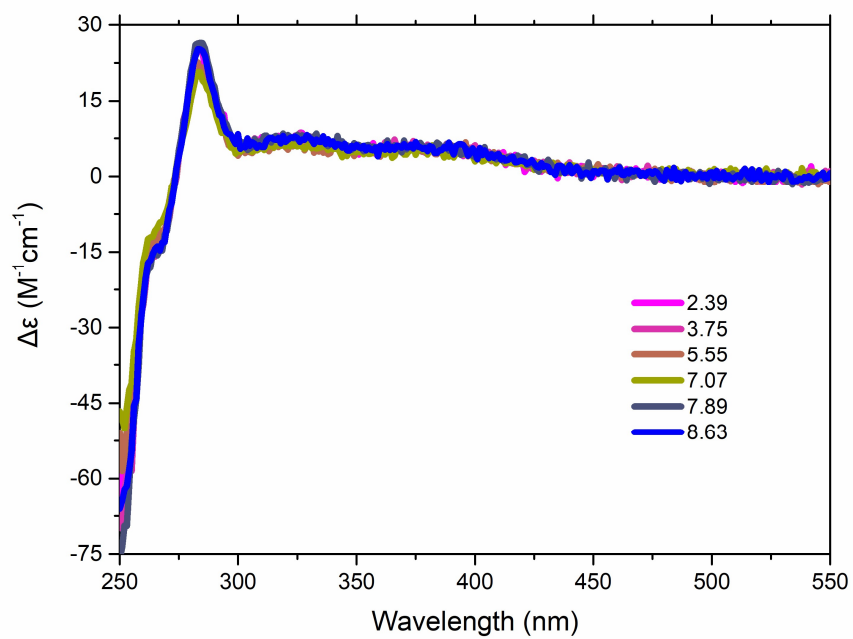


Figure S11. CD spectrum of P2 (20 μM) in solution with different pH value.

¹H NMR and ¹³C NMR Spectra.

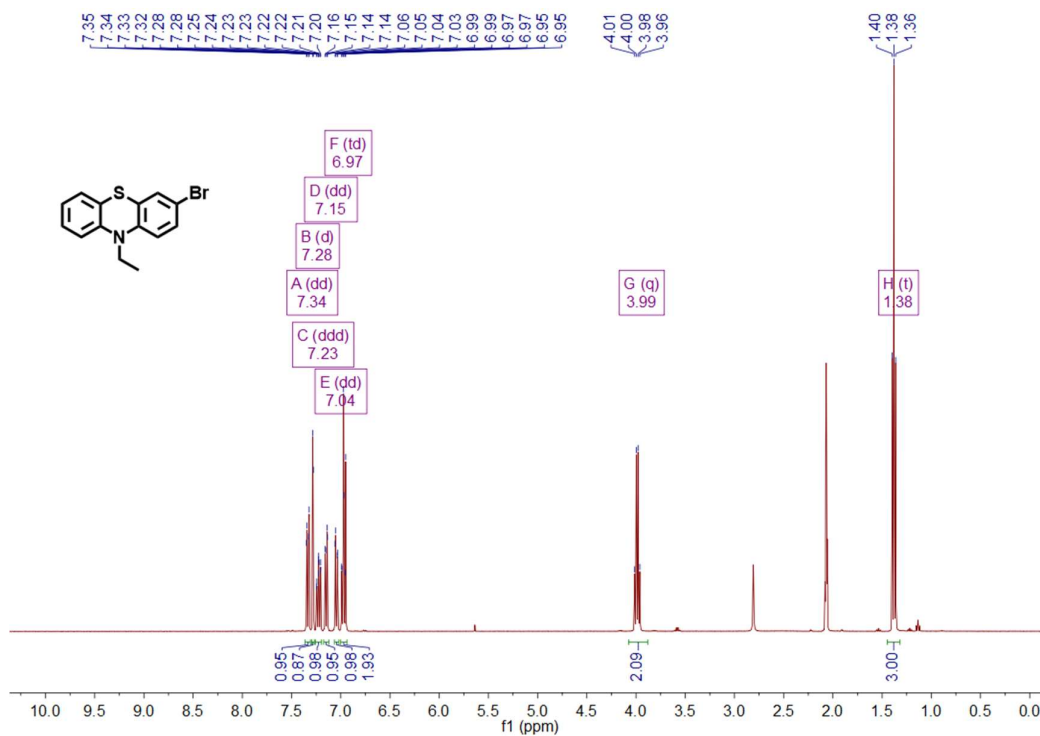


Figure S12. ¹H NMR spectrum of 1 in acetone-d₆.

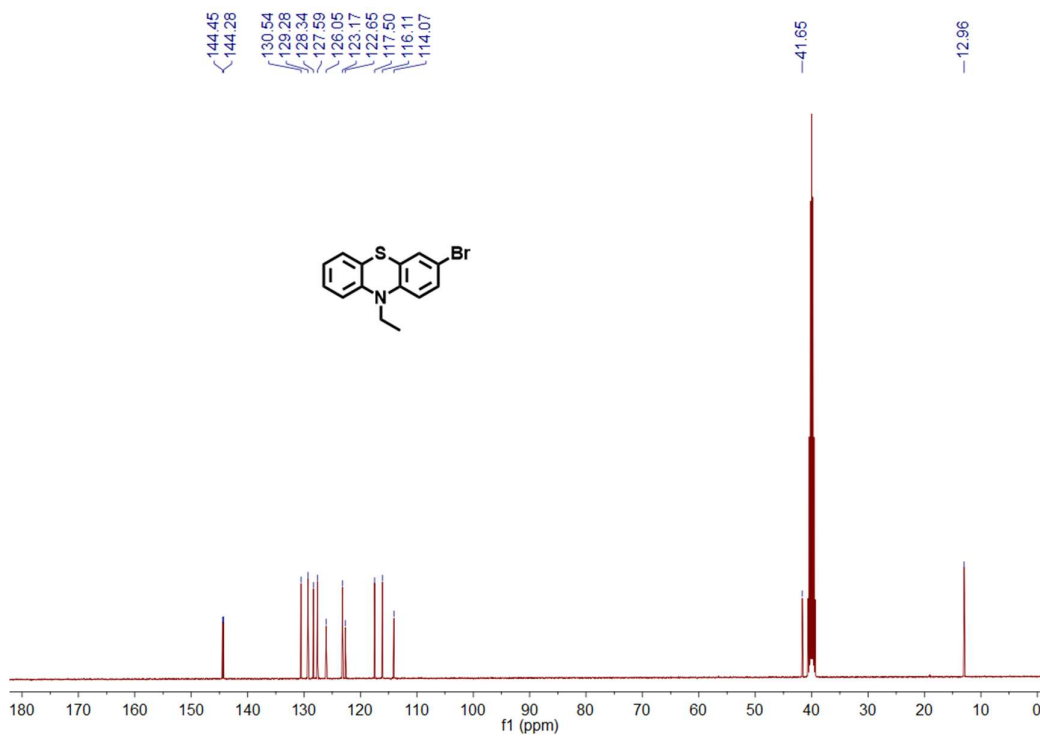


Figure S13. ¹³C NMR spectrum of 1 in DMSO-d₆.

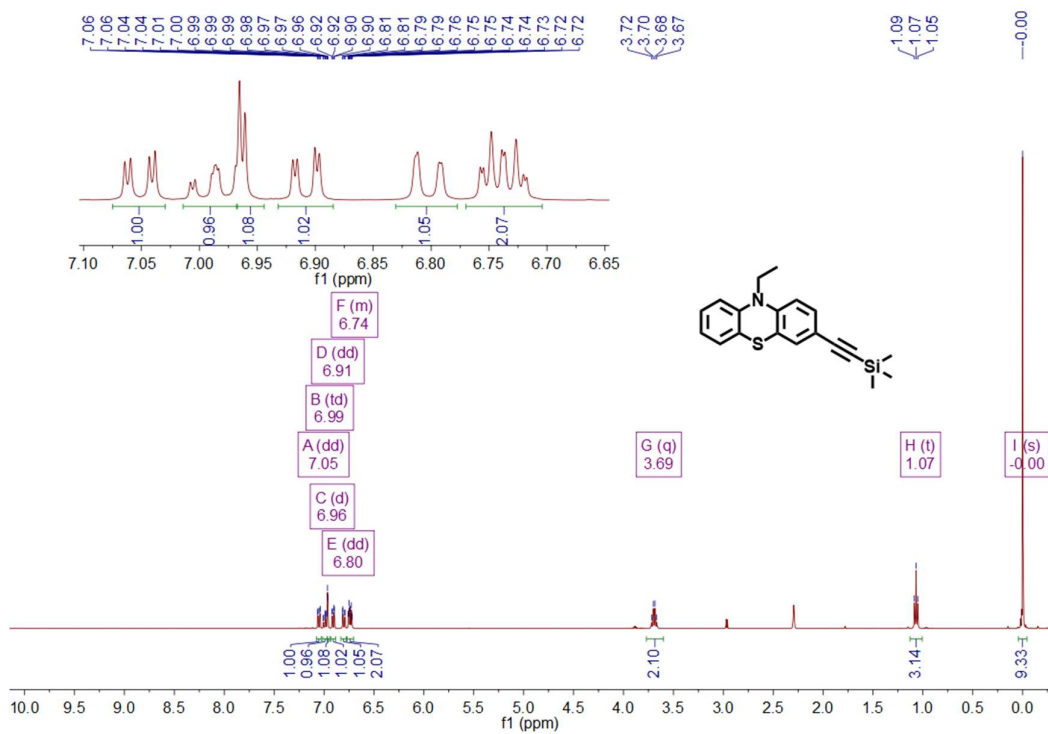


Figure S14. ^1H NMR spectrum of **2** in acetone- d_6 .

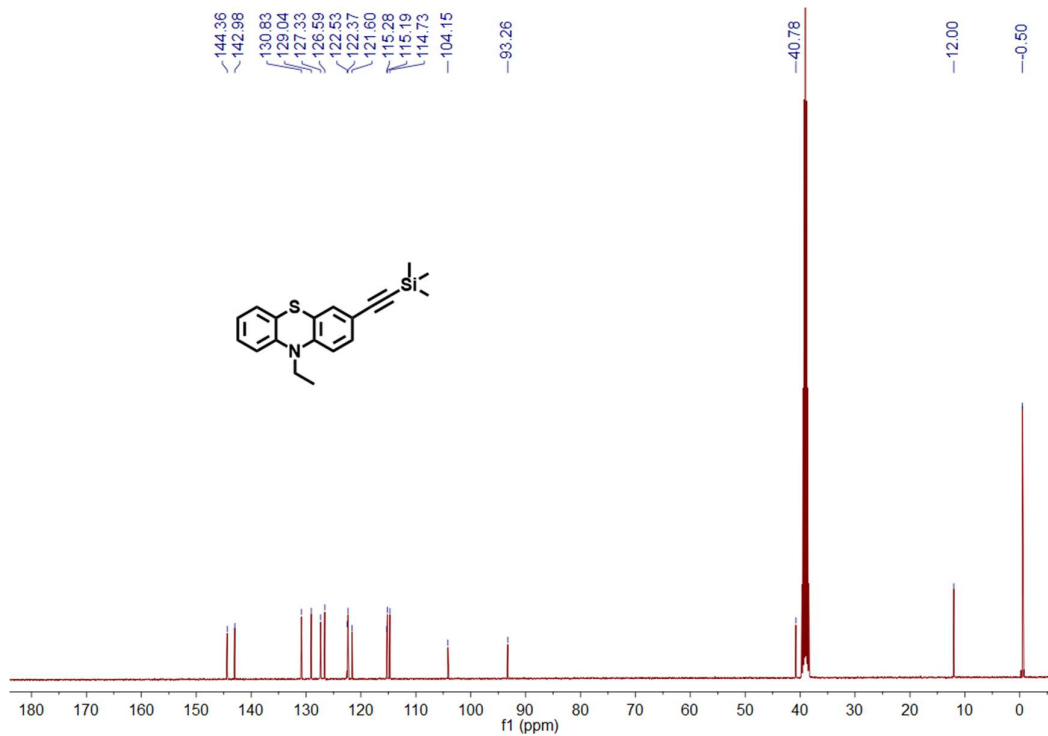


Figure S15. ^{13}C NMR spectrum of **2** in DMSO- d_6 .

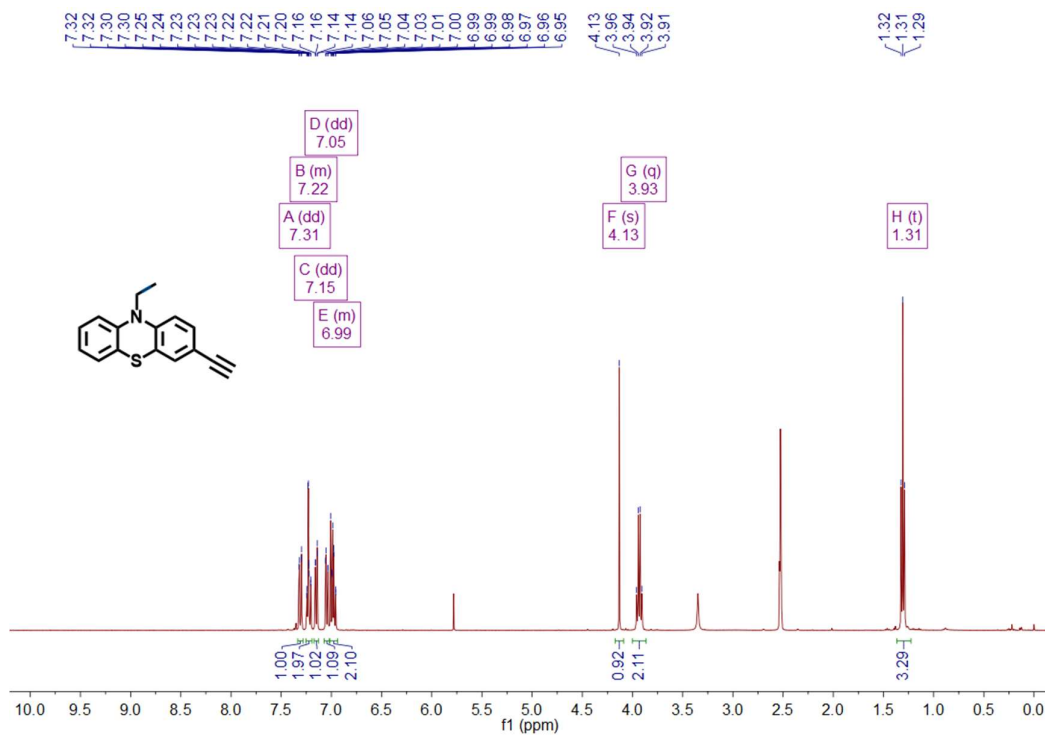


Figure S16. ¹H NMR spectrum of 3 in DMSO-d₆.

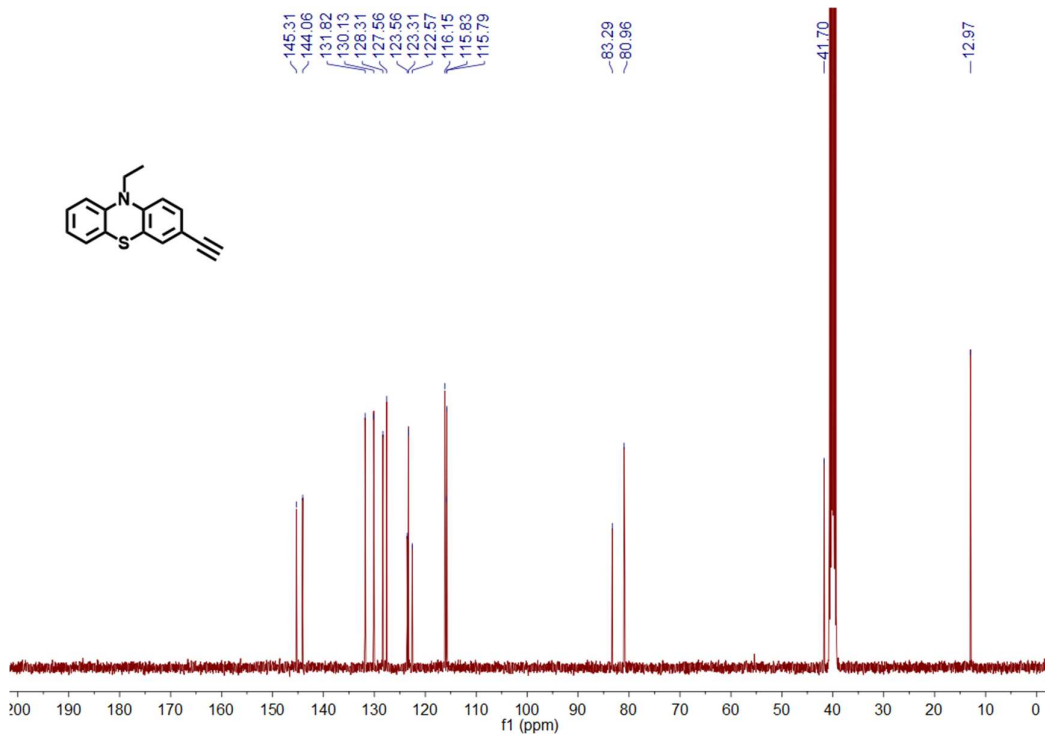


Figure S17. ¹³C NMR spectrum of 3 in DMSO-d₆.

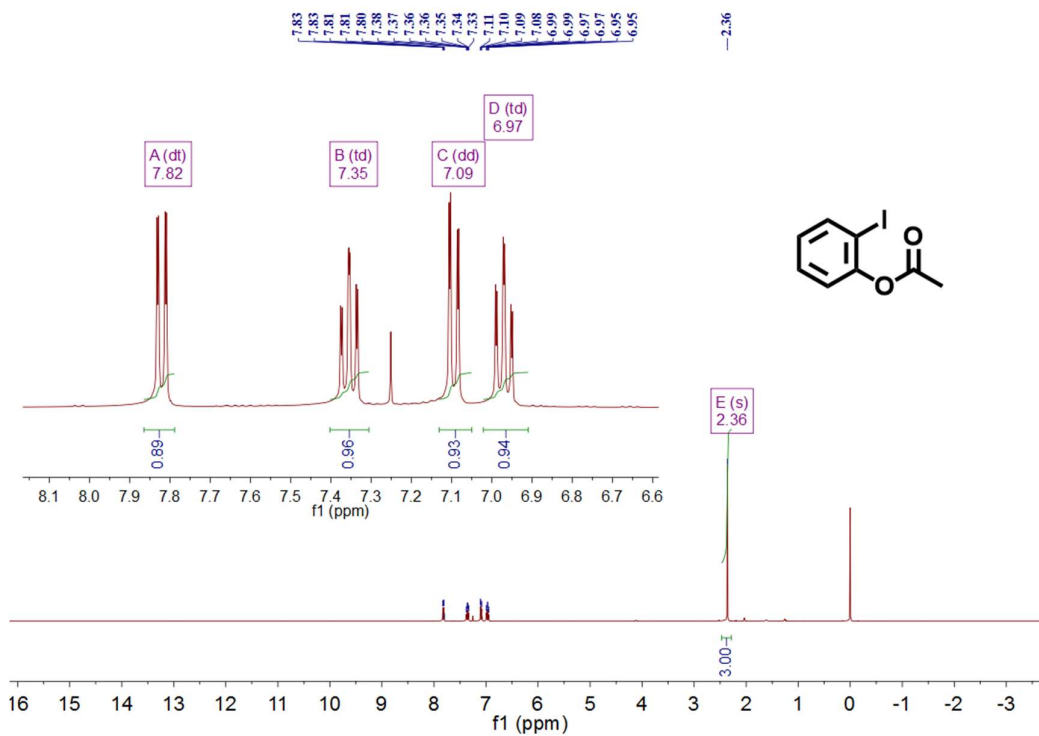


Figure S18. ¹H NMR spectrum of 4 in CDCl₃.

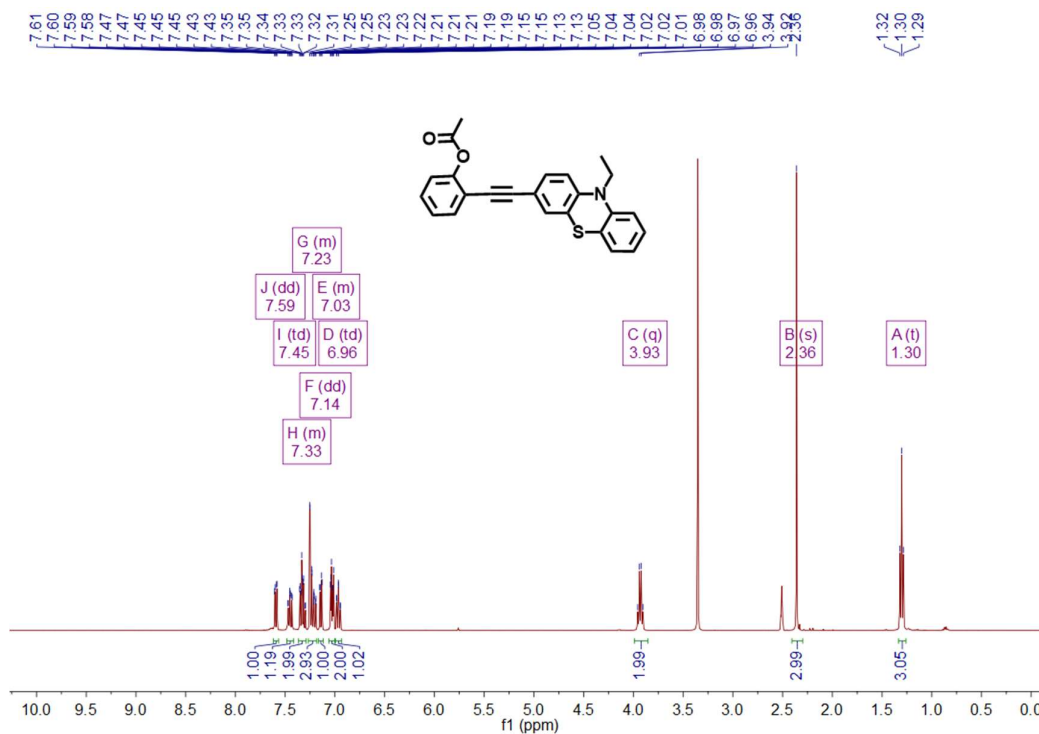


Figure S19. ¹H NMR spectrum of 5 in DMSO-d₆.

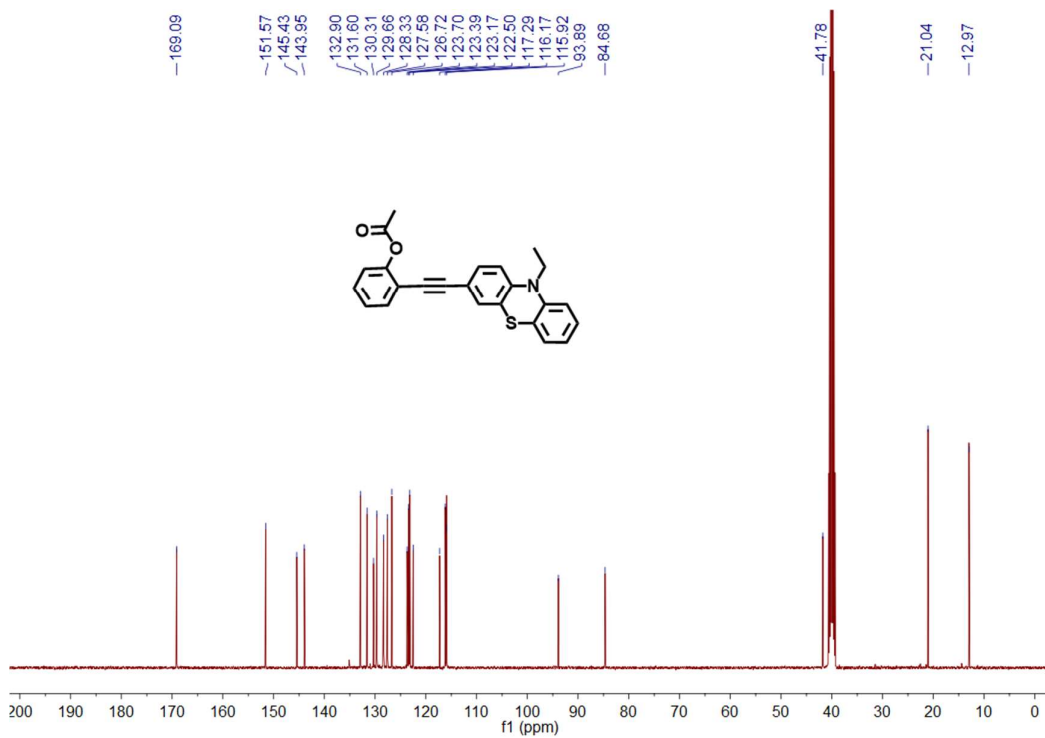


Figure S20. ¹³C NMR spectrum of **5** in DMSO-d₆.

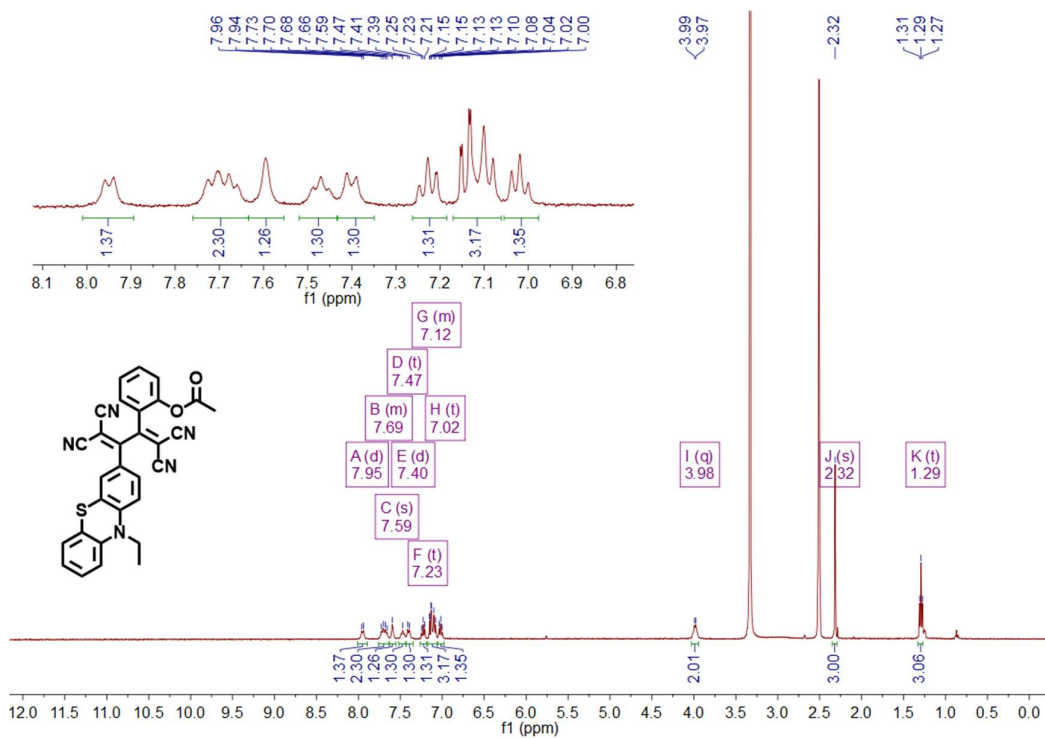


Figure S21. ¹H NMR spectrum of **6** in DMSO-d₆.

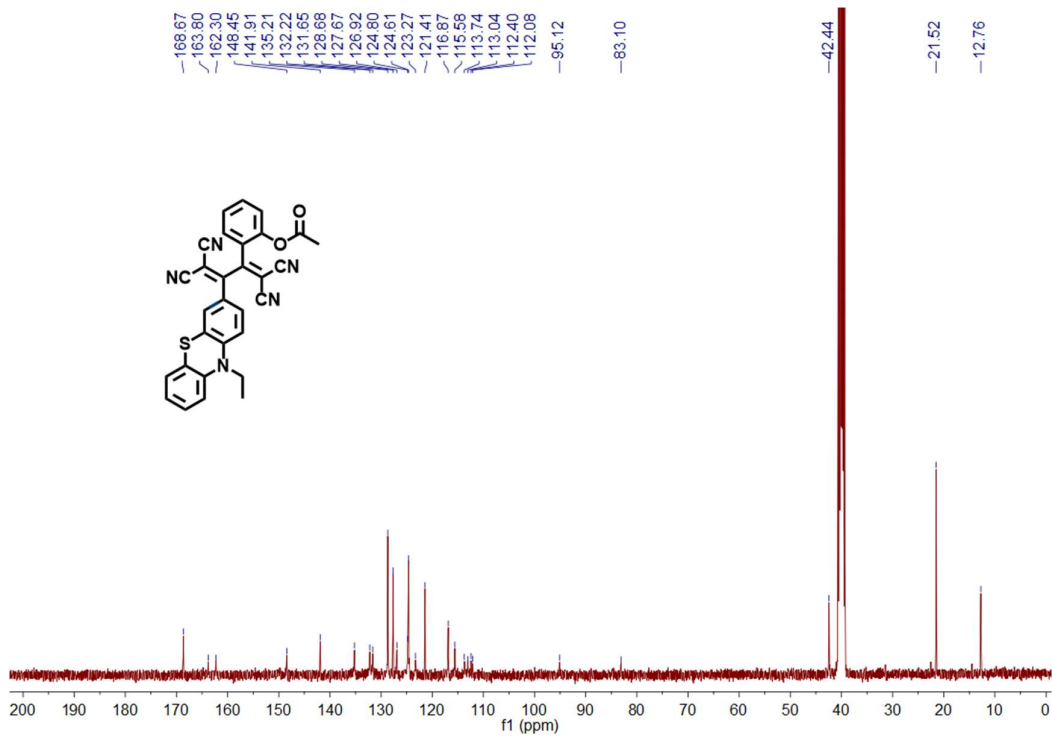


Figure S22. ¹³C NMR spectrum of 6 in DMSO-d₆.

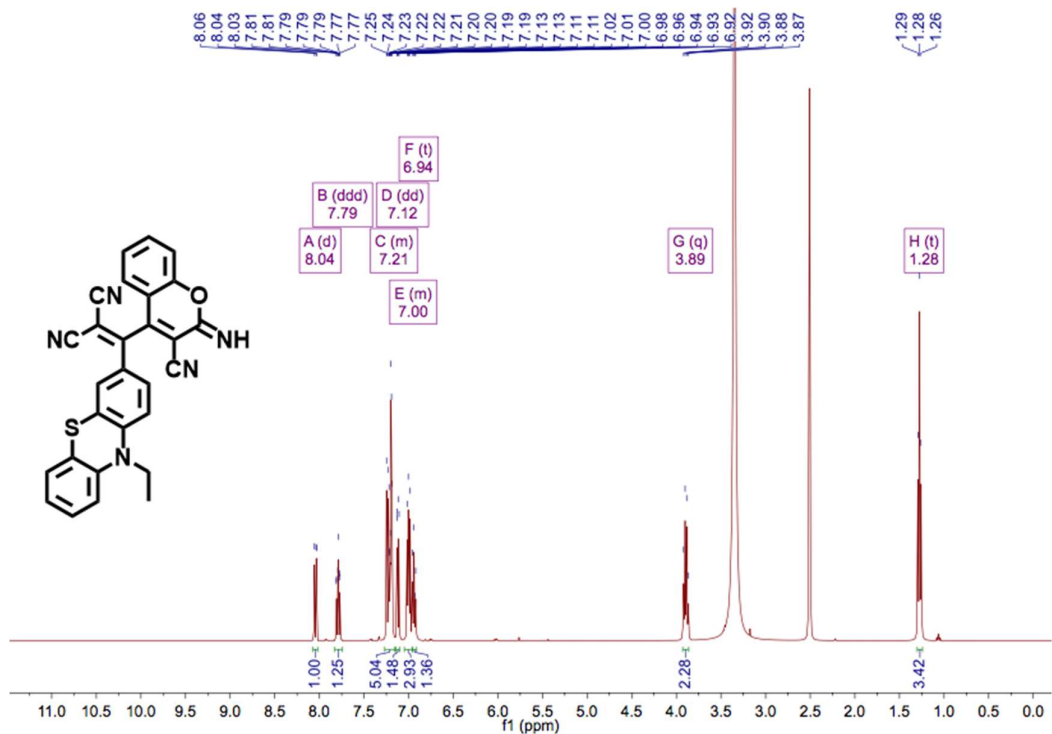


Figure S23. ¹H NMR spectrum of 7 in DMSO-d₆.

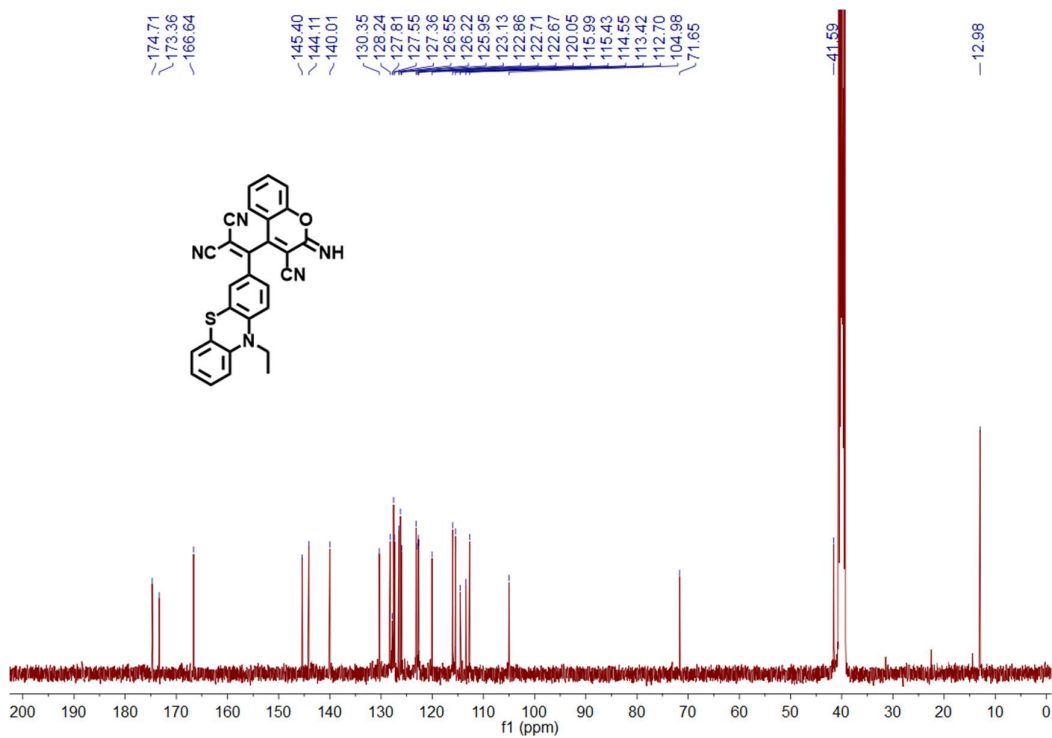


Figure S24. ¹³C NMR spectrum of 7 in DMSO-d₆.

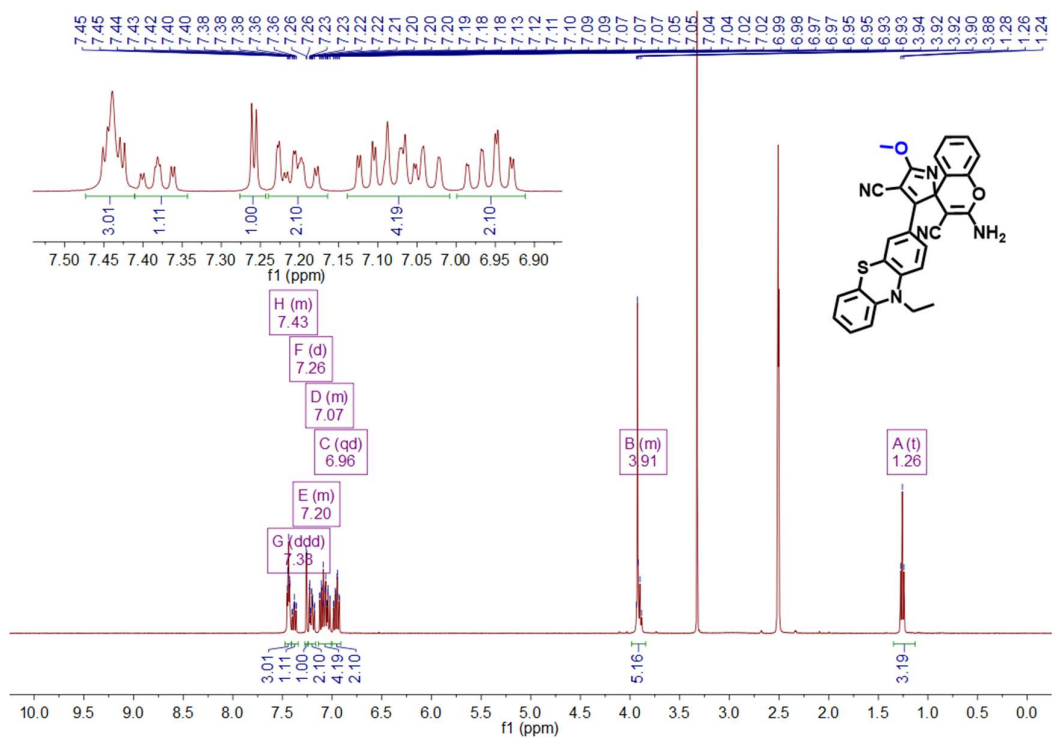


Figure S25. ¹H NMR spectrum of P in DMSO-d₆.

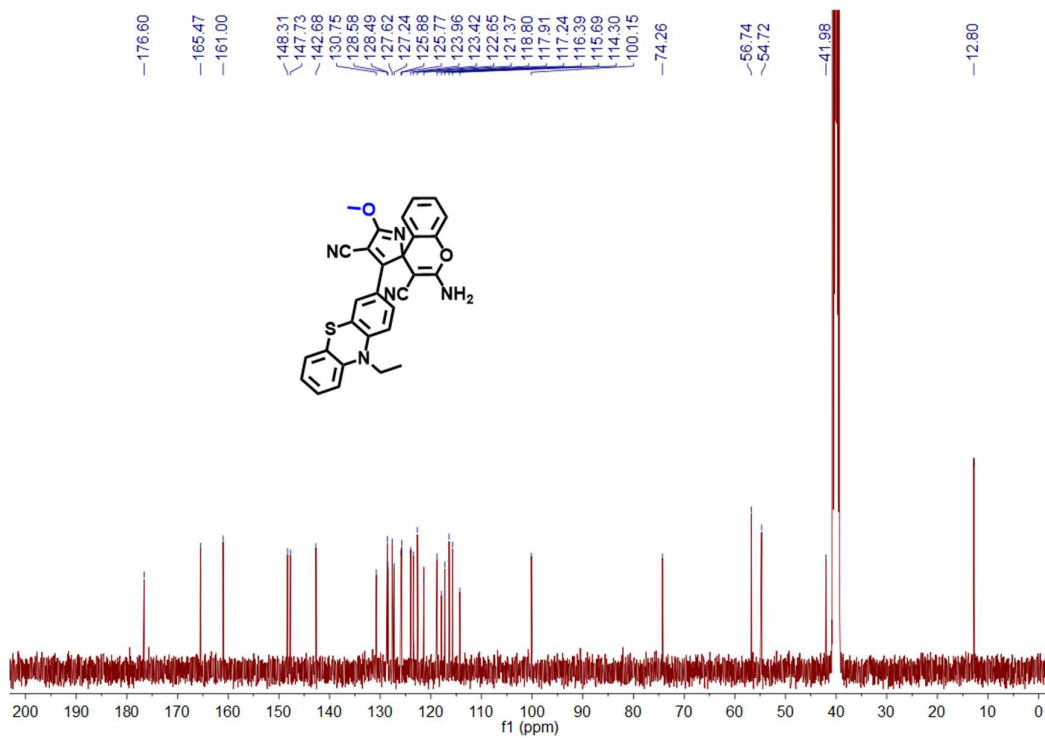


Figure S26. ^{13}C NMR spectrum of P in DMSO-d_6 .

MS spectra.

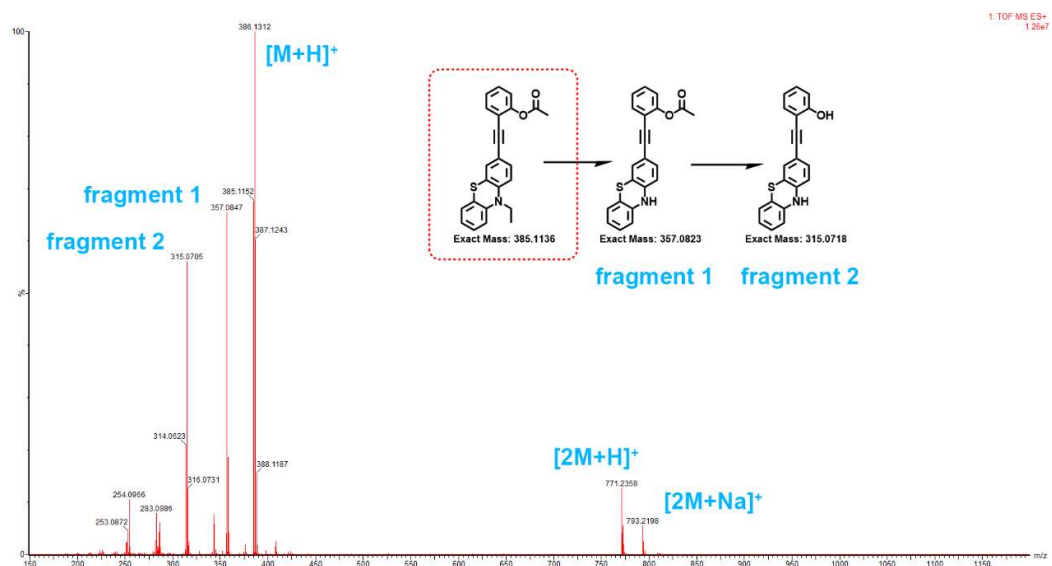


Figure S27. Mass spectra of 5.

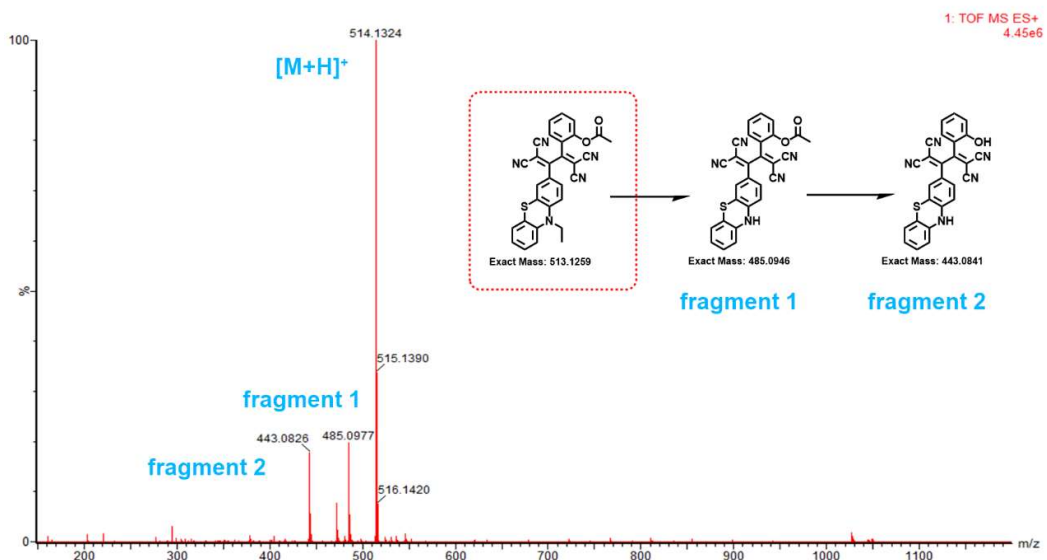


Figure S28. Mass spectra of 6.

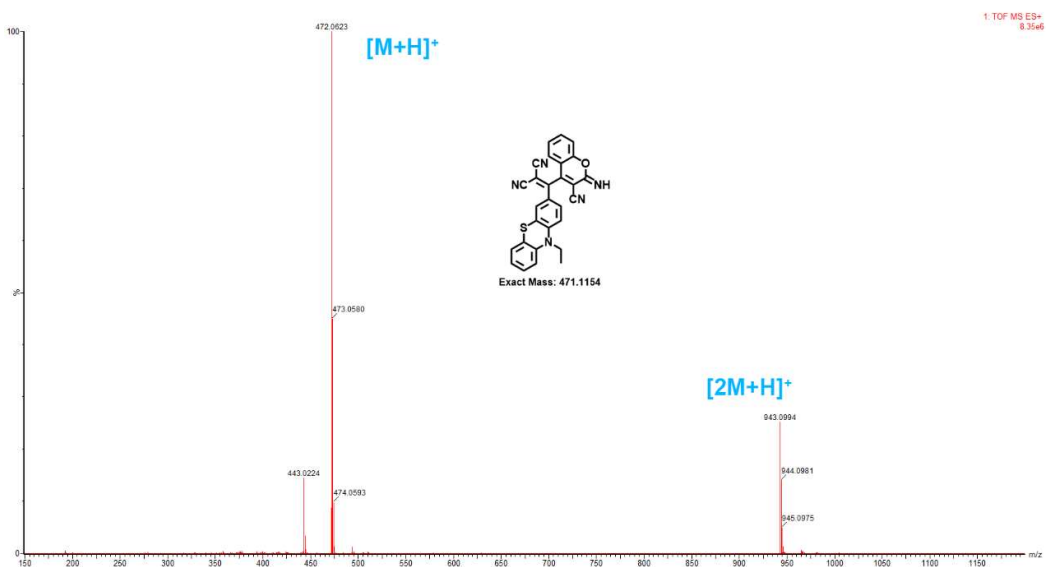


Figure S29. Mass spectra of 7.

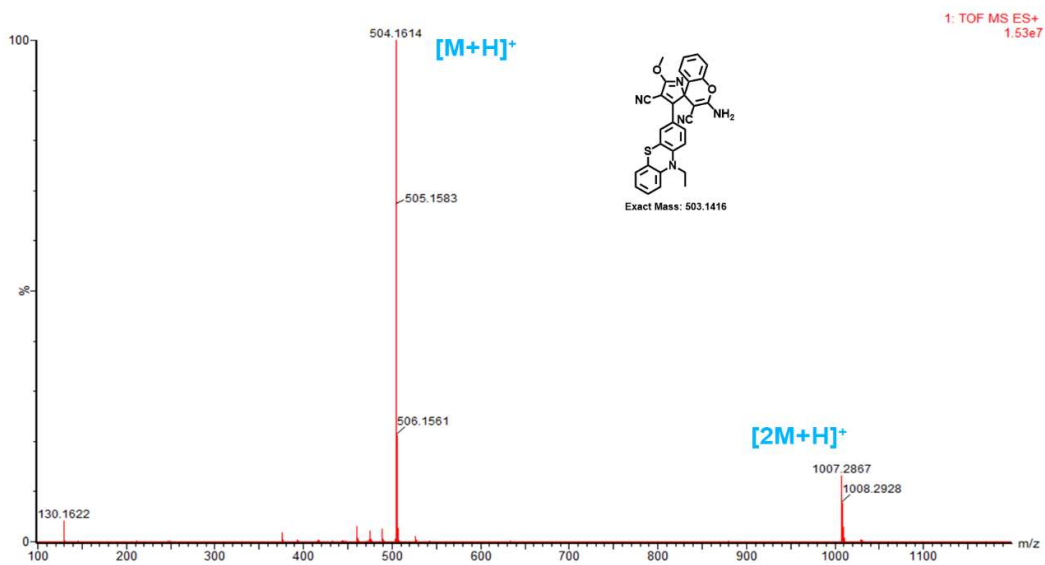


Figure S30. Mass spectra of P.

References

- [1] a) W. Kuhn, *Transactions of the Faraday Society* **1930**, *26*, 293-308; b) M. Wakabayashi, S. Yokojima, T. Fukaminato, K.-i. Shiino, M. Irie, S. Nakamura, *The Journal of Physical Chemistry A* **2014**, *118*, 5046-5057.
- [2] A. Chandrasekhar, V. Ramkumar, S. Sankararaman, *Eur. J. Org. Chem.* **2016**, *2016*, 4041-4049.